

Mononuclear Pseudostannatranes Possessing Unsymmetrical [4.4.3.0^{1,5}]Tridecane Cage: Experimental and Theoretical Aspects of Reverse Kocheshkov Reaction in Phenyl Pseudostannatrane

Keshav Kumar, Neha Srivastav, Mayank Khara, Neetu Goel, Raghubir Singh,* and Varinder Kaur*

Cite This: *Inorg. Chem.* 2020, 59, 13098–13108

Read Online

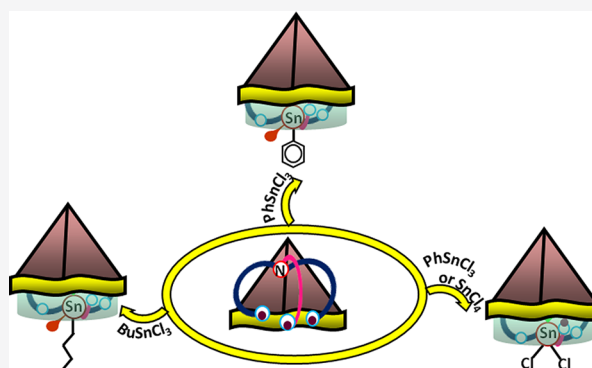
ACCESS |

Metrics & More

Article Recommendations

Supporting Information

ABSTRACT: The synthetic protocols, structural aspects, and spectroscopic aspects of mononuclear pseudostannatranes possessing a [4.4.3.0^{1,5}]tridecane cage have been reported. A tripodal ligand $N(\text{CH}_2\text{CH}_2\text{OH})\{\text{CH}_2(2-t\text{-Bu-4-Me-C}_6\text{H}_2\text{OH})\}_2$ (H_3L) having unsymmetrical arms was reacted with *n*-butyltrichlorostannane, phenyltrichlorostannane, and tin tetrachloride under different solvent systems to obtain pseudostannatranes (1–3). The reaction of *n*-butyltrichlorostannane and the ligand in $\text{CH}_3\text{OH}/\text{Na}/\text{THF}$ yielded an aqua complex of pseudostannatrane $[\text{LSnBu}(\text{H}_2\text{O})]$ (1_a), which was crystallized as its acetone solvate (i.e. $1_a \cdot \text{Me}_2\text{CO}$). However, the same reactants yielded methanol complex $[\text{LSnBu}(\text{CH}_3\text{OH})]$ (1_b) when the reaction was carried out in the $\text{NaOCH}_3/\text{C}_2\text{H}_5\text{OH}$ system. Similarly, the reaction of phenyltrichlorostannane and the ligand under these solvent systems yielded pseudostannatranes, i.e., an aqua complex $[\text{LSnPh}(\text{H}_2\text{O})]$ (2_a) and a methanol complex $[\text{LSnPh}(\text{CH}_3\text{OH})]$ (2_b) (where 2_a was crystallized as $2_a \cdot \text{Me}_2\text{CO}$). The reaction of tin tetrachloride and the ligand in the $\text{Et}_3\text{N}/\text{THF}$ system resulted in the formation of pseudostannatrane $[\text{LHSnCl}_2]$ (3). A similar product was isolated as its triethylamine solvate ($3 \cdot \text{NET}_3$) due to the disproportionation reaction when PhSnCl_3 was reacted with the ligand in the $\text{Et}_3\text{N}/\text{C}_6\text{H}_5\text{CH}_3$ system, which demonstrates the first report on the reverse Kocheshkov reaction in pseudostannatranes. The experimental findings on the formation of $3 \cdot \text{NET}_3$ due to the reverse Kocheshkov reaction have been corroborated with ^{119}Sn NMR spectroscopy and density functional calculations that provide insightful information about the underlying details of the reaction route.



INTRODUCTION

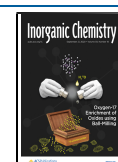
Over recent years, there has been growing interest in the synthesis and structural investigation of tin(IV) tricyclic compounds having $\text{N} \rightarrow \text{Sn}$ transannular interactions.^{1–8} Among the fused organotin tricycles, molecules having five-membered rings with a [3.3.3.0^{1,5}]undecane cage are termed “stannatranes,” while molecules containing rings other than five-membered arms are named “pseudostannatranes.”^{2,9–12} These structures are distinguished by their cage-like structure inclusive of right- or left-handed (Δ and Λ) propeller type geometry and an intramolecular $\text{N} \rightarrow \text{Sn}$ bond.^{13–15} Various stannatranes with general formula $\text{N}(\text{CH}_2\text{CH}_2\text{X})_3\text{SnR}$ (where $\text{X} = \text{O}, \text{S}, \text{NMe}, \text{CH}_2$; $\text{R} = \text{alkyl/aryl}$) and $\text{N}\{\text{CH}_2\text{C}(\text{O})\text{X}\}_3\text{SnR}$ (where $\text{X} = \text{O}$ or NMe) have been reported in the past.^{2,16–22} Their popularity has led to the syntheses of organic compounds and drug carbapenem from $\text{N}(\text{CH}_2\text{CH}_2\text{CH}_2)_3\text{SnR}$ due to selective reactivity of the $\text{Sn}-\text{R}$ bond.^{23–28} In addition, purely inorganic (lacking $\text{Sn}-\text{C}$ bond) stannatranes are also known and have been recently reported by Jurkschat et al.^{6–8,15,29} On the contrary, known pseudostannatranes have unsymmetrical [4.3.3.0^{1,5}]dodecane and [4.4.3.0^{1,5}]tridecane

cages with oligomeric structures formed via $\text{Sn}-\text{O}$ bridges and a symmetrical [4.4.4.0^{1,6}]tetradecane cage as a mononuclear entity.^{3,4,29} To the best of our knowledge, pseudostannatranes possessing a [4.4.3.0^{1,5}]tridecane cage as mononuclear entities have not been reported yet.

The interest in stannatrane-like molecules is driven by the fact that they are a prerequisite for breakthrough applications influencing basic organic synthesis, polymerization reactions, and polyurethane formation; therefore they are essential for the chemical and medicinal industries.^{30–34} The biggest obstacle for the exploration of stannatranes in multiple applications is the oligomerization of mononuclear entities during reaction via reactive groups/atoms present in the ligating system.^{6,17,29} Therefore, it is desirable to engineer new

Received: April 24, 2020

Published: September 9, 2020



skeletons of tin(IV) with sufficient architectural patterns to suppress oligomerization.

In our previous attempts to obtain pseudostannatranes from a tripodal unsymmetrical ligand, we obtained oligomeric structures in a solid as well as in a solution phase due to the flexibility of one of the arms of the ligand which provided space for μ -oxo bridges.⁴ Herein, we utilized a heteropolydentate ligand $N(\text{CH}_2\text{CH}_2\text{OH})\{\text{CH}_2(2-t\text{-Bu-4-Me-C}_6\text{H}_2\text{OH})\}_2$ (H_3L) with a bulky substituent in the phenolic ring to obtain pseudostannatranes. The H_3L is previously reported to obtain dinuclear complexes of iron and vanadium, Fe_2L_2 and $\text{V}_2\text{O}_2\text{L}_2$, respectively (where L is deprotonated ligand).^{35–37} Although the structure of its analog, i.e., $N(\text{CH}_2\text{CH}_2\text{OMe})\{\text{CH}_2(2-t\text{-Bu-4-Me-C}_6\text{H}_2\text{OH})\}_2$ (having variation at the alcoholic arm), has been investigated,³⁸ structural aspects of the H_3L , however, were not elucidated in detail. In the present work, the H_3L has been isolated in crystalline form, and its structure is confirmed by spectroscopic studies and single-crystal X-ray crystallography. It is reacted with tin precursors in varying solvent systems to obtain pseudostannatranes. The structures of pseudostannatranes are elucidated by elemental studies, spectroscopic studies, spectrometric studies, and single-crystal X-ray crystallography. The compounds are found to be mononuclear $[4.4.3.0^{1,5}]$ tridecane cages with hexacoordination at the Sn center. It is expected that *tert*-butyl groups present in the ligating system provide steric crowding around central metal and facilitate the formation of mononuclear entities. The formation of distinct products (i.e., $\mathbf{2}_{a/b}$ and $\mathbf{3-NEt}_3$) by the reaction of PhSnCl_3 and a ligand under different experimental conditions exemplifies the reverse Kocheshkov reaction. The mechanistic route for exceptional findings in the formation of $\mathbf{3-NEt}_3$ is justified based on spectroscopic studies of the reaction mixture at different intervals, computational studies, and literature reports. Previously, the reverse Kocheshkov reaction is reported in organostannanes, alkyl and aryl tin species, and organotin(IV) complexes; however, the formation of $\mathbf{3-NEt}_3$ is the first report on the reverse Kocheshkov reaction in the family of stannatranes.^{39–44}

EXPERIMENTAL SECTION

Materials. Synthesis of all the compounds was carried out using the Schlenk technique under dry nitrogen. Commercially purchased solvents were dried and stored under nitrogen. Triethylamine (CDH) was distilled over KOH pellets before use. Other chemicals, 2-(*t*-butyl)-4-methylphenol (Acros), formaldehyde (Aldrich), ethanolamine (Acros), *n*-butyltrichlorostannane (Acros), phenyltrichlorostannane (Aldrich), and tin tetrachloride (Aldrich), were used without any further purification.

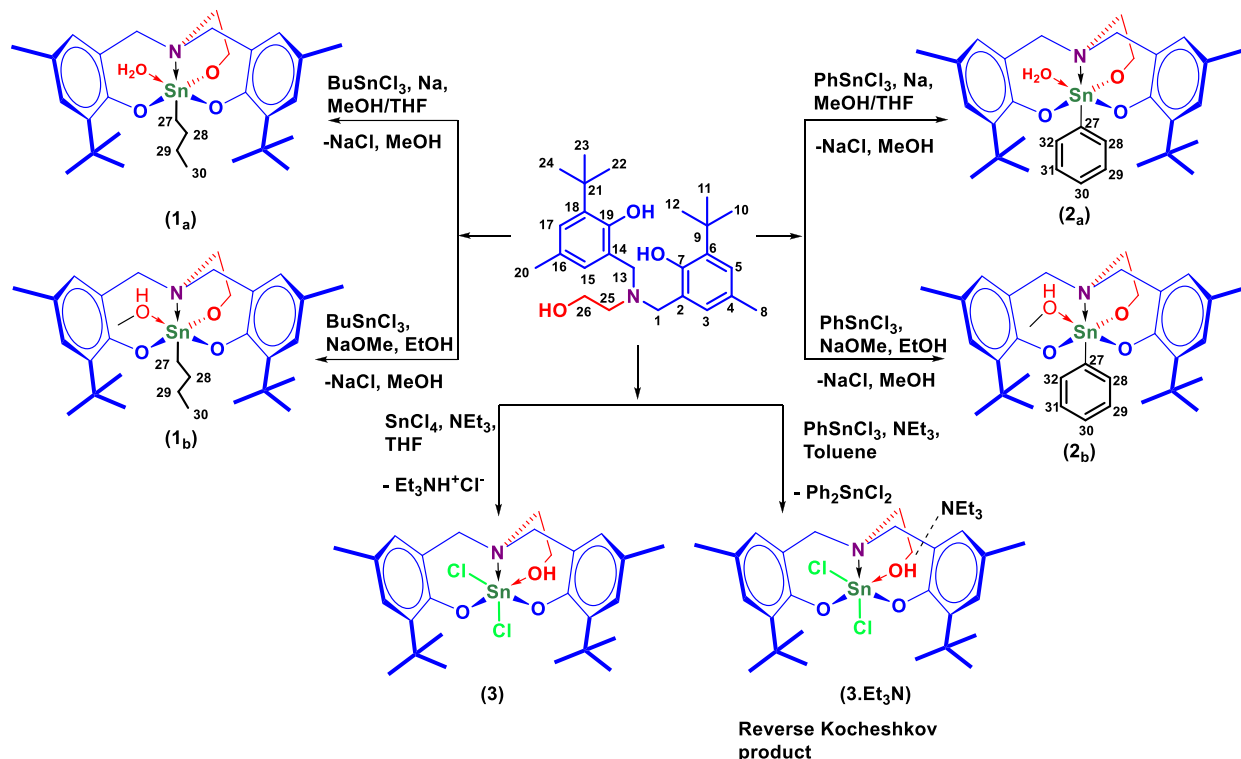
Physical Measurements. A Thermo Scientific Nicolet ISS0 FT-IR spectrometer was used to record the FT-IR spectra in the solid state. Mass spectra were recorded with a Xevo G2-XS QTOF spectrometer and VG Analytical (70-S) Spectrometer. A Flash-2000 organic elemental analyzer was used for C, H, and N elemental microanalyses. Solution NMR spectra were recorded at 25 °C on a Bruker Avance II FT NMR (AL 400 MHz) or Bruker Avance II FT NMR (AL 500 MHz) or Jeol JNM ECS400 (400 MHz) spectrometer (^1H , ^{13}C , ^{119}Sn). Chemical shifts are reported in parts per million relative to tetramethylsilane (TMS) for ^1H and ^{13}C and tetramethylstannane for ^{119}Sn NMR. A Rigaku XTA Lab SuperNova, single source (Mo $K\alpha$, $\lambda = 0.71073$) at offset/far, HyPix3000 diffractometer was used to collect crystallographic data. The crystal was kept at 293(2) K during data collection. The structure was solved using Olex2 with the ShelXT structure solution program using intrinsic phasing and refined with the ShelXL refinement package using least squares minimization.^{45–47} The reaction mechanism has been

investigated by performing geometry optimizations followed by frequency calculations within the formalism of density functional theory (DFT). Hybrid exchange-correlation functional B3LYP in conjunction with/6-31+G (d,p) and LanL2DZ as implemented in the Gaussian 09 package is the employed level of theory.^{48–51}

Syntheses. H_3L : $N(\text{CH}_2\text{CH}_2\text{OH})\{\text{CH}_2(2-t\text{-Bu-4-Me-C}_6\text{H}_2\text{OH})\}_2$. The ligand H_3L was synthesized by Mannich condensation reaction. Briefly, starting reagents 2-(*t*-butyl)-4-methylphenol (3.28 g, 20.00 mmol), aqueous formaldehyde (37%, 1.63 g, 20.00 mmol), and 2-aminoethanol (0.61 g, 10.00 mmol) were heated at reflux in methanol (30 mL) for 24 h to afford a clear solution. The solvent was evaporated, and the resulting oil was dissolved in toluene. The contents were left to stand at room temperature, which gave crystals suitable for X-ray crystallography. Yield: 85% (3.51 g, 8.50 mmol). Melting point: 75 °C. Elemental analysis calculated for $\text{C}_{26}\text{H}_{39}\text{NO}_3$: C, 75.50; H, 9.50; N, 3.39. Found: C, 75.30; H, 9.58; N, 3.31. FT-IR (cm^{-1}): 1476 (C=C, phenyl ring), 1605 (C=C, phenyl ring), 2864, 2913, 2952 (C–H), 3391 br, 3581 (O–H). ^1H NMR (400 MHz, CDCl_3): δ (ppm) 1.38 (s, $18\text{H}^{10-12,22-24}$), 2.22 (s, $6\text{H}^{8,20}$), 2.68 (t, 2H^{25} , $^3\text{J}(\text{H}^1-\text{H}^1) = 5.2$ Hz), 3.70 (s, $4\text{H}^{1,13}$), 3.79 (t, 2H^{26} , $^3\text{J}(\text{H}^1-\text{H}^1) = 5.2$ Hz), 6.71 (d, $2\text{H}^{3,15}$, $^4\text{J}(\text{H}^1-\text{H}^1) = 1.6$ Hz), 6.99 (d, $2\text{H}^{5,17}$, $^4\text{J}(\text{H}^1-\text{H}^1) = 1.6$ Hz), 8.10 (br, 1H, CH_2OH). ^{13}C NMR (100 MHz, CDCl_3): δ (ppm) 20.7 ($\text{C}^{8,20}$), 29.6 ($\text{C}^{10-12,22-24}$), 34.6 ($\text{C}^{9,21}$), 53.7 (C^{25}), 57.4 ($\text{C}^{1,13}$), 61.2 (C^{26}), 122.4 ($\text{C}^{2,14}$), 127.3 ($\text{C}^{5,17}$), 127.7 ($\text{C}^{3,15}$), 128.8 ($\text{C}^{4,16}$), 136.8 ($\text{C}^{6,18}$), 152.8 ($\text{C}^{7,19}$). MS: m/z 414.30 $[\text{M} + \text{H}]^+$.

$(\mathbf{1}_a \cdot \text{Me}_2\text{CO})$: $[(N(\text{CH}_2\text{CH}_2\text{O})\{\text{CH}_2(2-t\text{-Bu-4-Me-C}_6\text{H}_2\text{O})\}_2)\text{Sn}(n\text{-Bu})(\text{H}_2\text{O})] \cdot (\text{Me}_2\text{CO})$. To the ligand H_3L (0.83 g, 2.00 mmol), freshly prepared sodium methoxide solution (0.14 g, 6.00 mmol of sodium metal in 10 mL of methanol) was added. The solution was heated at reflux for 1 h and diluted with 20 mL of THF. The resultant solution was transferred dropwise to a solution of *n*-butyltin trichloride (0.33 mL, 2.00 mmol) in THF (20 mL) and heated at reflux for 1 h. The reaction mixture was filtered to separate sodium chloride, and the filtrate was evaporated under a vacuum to remove the solvent. The solid obtained was dissolved in dichloromethane (10 mL) and filtered again to remove solid impurity (if any). The contents were evaporated to dryness in vacuo to afford a solid. The resulting solid was dissolved in acetone, which, after slow evaporation, resulted in colorless blocked crystals of acetone solvate of the aqua complex of pseudostannatranane $\mathbf{1}$ ($\mathbf{1}_a \cdot \text{Me}_2\text{CO}$). Melting point: 221 °C. Yield: 84% (0.99 g, 1.68 mmol). Elemental analysis calculated for $\text{C}_{33}\text{H}_{53}\text{NO}_3\text{Sn}$: C, 59.83; H, 8.06; N, 2.11. Found: C, 59.67; H, 7.97; N, 2.04. FT-IR (cm^{-1}): 440 (Sn–N), 496 (Sn–O), 520 (Sn–C), 1466 (C=C, phenyl ring), 1609 (C=C, phenyl ring), 1705 (C=O, acetone), 2868, 2913, 2954 (C–H), 3292 (O–H). ^1H NMR (400 MHz, $\text{DMSO}-d_6$): δ (ppm) 0.92 (t, 3H^{30} , $^3\text{J}(\text{H}^1-\text{H}^1) = 7.2$ Hz), 1.30–1.38 (m, $22\text{H}^{10-12,22-24,27,29}$), 1.76–1.84 (m, 2H^{28}), 2.14 (s, $6\text{H}^{8,20}$), 2.67 (t, 2H^{25} , $^3\text{J}(\text{H}^1-\text{H}^1) = 5.6$ Hz), 3.00 (t, 2H^{26} , $^3\text{J}(\text{H}^1-\text{H}^1) = 5.6$ Hz), 3.60 (d, $2\text{H}^{1,13}$, $^2\text{J}(\text{H}^1-\text{H}^1) = 12.0$ Hz), 4.34 (d, $2\text{H}^{1,13}$, $^2\text{J}(\text{H}^1-\text{H}^1) = 12.0$ Hz), 6.66 (d, $2\text{H}^{3,15}$, $^4\text{J}(\text{H}^1-\text{H}^1) = 1.8$ Hz), 6.86 (d, $2\text{H}^{5,17}$, $^4\text{J}(\text{H}^1-\text{H}^1) = 1.8$ Hz). ^{13}C NMR (100 MHz, $\text{DMSO}-d_6$): δ (ppm) 13.6 (C^{30}), 20.4 (C^{27}), 22.7 (C^{28}), 26.6 ($\text{C}^{8,20}$), 27.4 (C^{29}), 34.1 ($\text{C}^{10-12,22-24}$), 34.1 ($\text{C}^{9,21}$), 48.2 ($\text{C}^{1,13}$), 59.3 (C^{25}), 61.9 (C^{26}), 122.4 ($\text{C}^{2,14}$), 122.9 ($\text{C}^{5,17}$), 126.9 ($\text{C}^{3,15}$), 128.6 ($\text{C}^{4,16}$), 137.4 ($\text{C}^{6,18}$), 159.5 ($\text{C}^{7,19}$). ^{119}Sn NMR (149 MHz, $\text{DMSO}-d_6$): δ (ppm) –476. MS: m/z 414.31 $[\text{L} + \text{H}]^+$, 588.26 $[\text{M} + \text{H}]^+$.

$\mathbf{1}_b$: $[(N(\text{CH}_2\text{CH}_2\text{O})\{\text{CH}_2(2-t\text{-Bu-4-Me-C}_6\text{H}_2\text{O})\}_2)\text{Sn}(n\text{-Bu})(\text{MeOH})]$. The ligand H_3L (0.41 g, 1.00 mmol) and sodium methoxide (0.16 g, 3.00 mmol) were dissolved in 30 mL of ethanol with stirring for 15 min. A solution of *n*-butyltin trichloride (0.16 mL, 1.00 mmol) in 10 mL of ethanol was added dropwise over a period of 20 min at room temperature. The mixture was stirred for 6 h. The solvent was removed in a vacuum, and dichloromethane (10 mL) was added to dissolve the residue. The solid impurities were filtered and the filtrate was reduced to 1/2 volumes. Then, 5 mL of ethanol was added to the concentrated solution and left to stand for a few days, which yielded crystals of pseudostannatranane $\mathbf{1}_b$ as colorless blocks. Melting point: 218 °C. Yield: 88% (0.51 g, 0.88 mmol). Elemental analysis calculated for $\text{C}_{31}\text{H}_{49}\text{NO}_4\text{Sn}$: C, 60.21; H, 7.99; N, 2.26. Found: C, 60.04; H,

Scheme 1. Reaction Scheme to Obtain Pseudostannatranes (**1_a**, **1_b**, **2_a**, **2_b**, **3**, and **3·Et₃N**)^a

^aThe numbers on the structural skeletons refer to the assignment of the NMR data.

7.84; N, 2.17. FT-IR ν (cm^{-1}): 441 (Sn–N), 496 (Sn–O), 519 (Sn–C), 1467 (C=C, phenyl ring), 1605 (C=C, phenyl ring), 2872, 2913, 2953 (C–H), 3224 (O–H). ¹H NMR (400 MHz, DMSO-*d*₆): δ (ppm) 0.94 (t, 3H³⁰, ³J(¹H–¹H) = 7.6 Hz), 1.28–1.41 (m, 22H^{10–12,22–24,27,29}), 1.79–1.87 (m, 2H²⁸), 2.15 (s, 6H^{8,20}), 2.69 (br, 2H²⁵), 3.03 (br, 2H²⁶), 3.44 (br, 3H, CH₃OH), 3.60 (d, 2H^{1,13}, ²J(¹H–¹H) = 8.0 Hz), 4.35 (d, 2H^{1',13'}, ²J(¹H–¹H) = 8.0 Hz), 6.67 (s, 2H^{3,15}), 6.88 (s, 2H^{5,17}). ¹³C NMR (100 MHz, DMSO-*d*₆): δ (ppm) 13.6 (C³⁰), 20.4 (C²⁷), 22.1 (C²⁸), 26.6 (C^{8,20}), 27.4 (C²⁹), 29.4 (C^{10–12,22–24}), 34.1 (C^{9,21}), 55.8 (C²⁵), 59.3 (C^{1,13}), 62.0 (C²⁶), 62.6 (CH₃OH), 122.3 (C^{2,14}), 122.9 (C^{5,17}), 126.9 (C^{3,15}), 128.6 (C^{4,16}), 137.5 (C^{6,18}), 159.4 (C^{7,19}). ¹¹⁹Sn NMR (149 MHz, DMSO-*d*₆): δ (ppm) –477. MS, *m/z* 415.31 [L + 2H]⁺, 588.20 [M + H]⁺.

(2_a·Me₂CO): [(N(CH₂CH₂O){CH₂(2-*t*-Bu-4-Me-C₆H₂O)}₂)Sn(Ph)(H₂O)](Me₂CO). The ligand H₃L (0.83 g, 2.00 mmol) and phenyltin trichloride (0.33 mL, 2.00 mmol) were reacted in the same way as mentioned above for pseudostannatranane **1_a**·Me₂CO. Melting point: 243 °C. Yield: 92% (1.12 g, 1.84 mmol). Elemental analysis calculated for C₃₅H₄₉NO₅Sn: C, 61.60; H, 7.24; N, 2.05. Found: C, 61.44; H, 7.12; N, 1.96. FT-IR ν (cm^{-1}): 452 (Sn–N), 501 (Sn–O), 534 (Sn–C), 1465 (C=C, phenyl ring), 1609 (C=C, phenyl ring), 1701 (C=O, acetone), 2876, 2913, 2949 (C–H), 3304 (O–H). ¹H NMR (400 MHz, DMSO-*d*₆): 1.26 (s, 18H^{10–12,22–24}), 2.09 (s, 6H^{8,20}), 2.86 (s, 2H²⁵), 3.20 (s, 2H²⁶), 3.78 (d, 2H^{1,13}, ²J(¹H–¹H) = 11 Hz), 4.31 (d, 2H^{1',13'}, ²J(¹H–¹H) = 11 Hz), 6.70 (s, 2H^{3,15}), 6.87 (s, 2H^{5,17}), 7.31–7.37 (m, 3H^{29–31}), 7.97 (d, 2H^{28,32}, ³J(¹H–¹H) = 6.4 Hz, ³J(¹H–¹¹⁹Sn) = 85.6, ³J(¹H–¹¹⁹Sn) = 98.4). ¹³C NMR (100 MHz, DMSO-*d*₆): δ (ppm) 20.4 (C^{8,20}), 29.5 (C^{10–12,22–24}), 34.1 (C^{9,21}), 59.1 (C²⁵), 61.6 (C^{1,13}), 61.7 (C²⁶), 123.4 (C^{2,14}), 126.6 (C^{5,17}), 126.9 (C³⁰), 127.2 (C^{29,31}), 128.6 (C^{3,15}), 129.0 (C^{4,16}), 136.2 (C^{28,32}), 136.4 (C^{6,18}), 137.9 (C²⁷), 159.2 (C^{7,19}). ¹¹⁹Sn NMR (149 MHz, DMSO-*d*₆): δ (ppm) –532. MS: *m/z* 414.31 [L+H]⁺, 608.23 [M + H]⁺, 686.25 [M+C₆H₅+2H]⁺.

2b: [(N(CH₂CH₂O){CH₂(2-*t*-Bu-4-Me-C₆H₂O)}₂)Sn(Ph)(MeOH)]. A similar procedure was adopted to that of pseudostannatranane **1_b** for the reaction of H₃L (0.41 g, 1.00 mmol) and phenyltin trichloride (0.16

mL, 1.00 mmol) in the presence of sodium methoxide (0.16 g, 3.00 mmol). Melting point: 239 °C. Yield: 89% (0.54 g, 0.89 mmol). Elemental analysis calculated for C₃₃H₄₅NO₄Sn: C, 62.08; H, 7.10; N, 2.19. Found: C, 61.91; H, 6.96; N, 2.04. FT-IR ν (cm^{-1}): 447 (Sn–N), 504 (Sn–O), 539 (Sn–C), 1465 (C=C, phenyl ring), 1613 (C=C, phenyl ring), 2859, 2900, 2945 (C–H), 3201 (O–H). ¹H NMR (400 MHz, DMSO-*d*₆): 1.27 (s, 18H^{10–12,22–24}), 2.16 (s, 6H^{8,20}), 2.86 (s, 2H²⁵), 3.40 (s, 2H²⁶), 3.79 (d, 2H^{1,13}, ²J(¹H–¹H) = 11.0 Hz), 4.14 (s, 3H, CH₃OH), 4.32 (d, 2H^{1',13'}, ²J(¹H–¹H) = 11.0 Hz), 6.71 (d, 2H^{3,15}, ⁴J(¹H–¹H) = 1.4 Hz), 6.89 (d, 2H^{5,17}, ⁴J(¹H–¹H) = 1.4 Hz), 7.30–7.38 (m, 3H^{29–31}), 7.99 (d, 2H^{28,32}, ³J(¹H–¹H) = 7.6 Hz, ³J(¹H–¹¹⁹Sn) = 87.6, ³J(¹H–¹¹⁹Sn) = 100.4). ¹³C NMR (100 MHz, DMSO-*d*₆): δ (ppm) 20.4 (C^{8,20}), 29.5 (C^{10–12,22–24}), 34.1 (C^{9,21}), 48.5 (CH₃OH), 59.1 (C²⁵), 61.7 (C^{1,13}), 62.0 (C²⁶), 122.5 (C^{2,14}), 123.4 (C^{5,17}), 127.0 (C³⁰), 127.2 (C^{29,31}), 128.1 (C^{3,15}), 128.6 (C^{4,16}), 136.2 (C^{28,32}), 137.9 (C^{6,18}), 147.1 (C²⁷), 159.2 (C^{7,19}). ¹¹⁹Sn NMR (149 MHz, DMSO-*d*₆): δ (ppm) –531. MS: *m/z* 414.31 [L+H]⁺, 530.19 [M–C₆H₅]⁺, 608.20 [M + H]⁺.

3: [(N(CH₂CH₂OH){CH₂(2-*t*-Bu-4-Me-C₆H₂O)}₂)SnCl₂]. The mixture of ligand H₃L (0.41 g, 1.00 mmol) and triethylamine (0.30 g, 3.00 mmol) in THF (30 mL) was stirred for about 10 min in an ice bath. Then, a solution of tin tetrachloride (0.12 mL, 1.00 mmol) in THF (10 mL) was added dropwise over a period of 20 min under ice cold conditions. The mixture was stirred for 5 h at room temperature and filtered to remove the salt (triethylammonium chloride). The filtrate was reduced under a vacuum and kept for crystallization. It yielded a powdered pseudostannatranane **3** after few days. Melting point: 206–209 °C. Yield: 89% (crude, 0.53 g, 0.89 mmol). Elemental analysis calculated for C₂₆H₃₇Cl₂NO₃Sn: C, 51.94; H, 6.20; N, 2.33. Found: C, 51.85; H, 6.14; N, 2.29. FT-IR ν (cm^{-1}): 457 (Sn–N), 503 (Sn–O), 1464 (C=C, phenyl ring), 1611 (C=C, phenyl ring), 2865, 2917, 2951 (C–H) 3385 (O–H). ¹H NMR (400 MHz, CDCl₃): 1.29 (s, 18H^{10–12,22–24}), 2.15 (s, 6H^{8,20}), 2.85 (t, 2H²⁵, ³J(¹H–¹H) = 5.0 Hz), 3.36 (t, 2H²⁶, ³J(¹H–¹H) = 5.0 Hz), 3.45 (d, 2H^{1,13}, ²J(¹H–¹H) = 10 Hz), 4.86 (d, 2H^{1',13'}, ²J(¹H–¹H) = 10 Hz), 6.54 (s, 2H^{3,15}), 7.02 (s, 2H^{5,17}). ¹³C NMR (100 MHz, CDCl₃): δ (ppm) 20.7 (C^{8,20}),

29.9 (C^{10–12,22–24}), 34.7 (C^{9,21}), 46.6 (C²⁵), 56.3 (C^{1,13}), 68.1 (C²⁶), 119.8 (C^{2,14}), 126.2 (C^{5,17}), 128.3 (C^{3,15}), 129.7 (C^{4,16}), 139.3 (C^{6,18}), 158.4 (C^{7,19}). ¹¹⁹Sn NMR (149 MHz, CDCl₃): δ (ppm) –565, –569, –625, –669. MS: *m/z* 414.31 [L+H]⁺, 530.18 [M–2Cl–H]⁺, 608.20 [M–2Cl+C₆H₅].

3·NEt₃: [(N(CH₂CH₂OH){CH₂(2-*t*-Bu-4-Me-C₆H₂O)}₂SnCl₂)]·NEt₃. The ligand H₃L (0.41 g, 1.00 mmol) and triethylamine (0.30 g, 3.00 mmol) were dissolved in toluene (30 mL) and stirred for 10 min in an ice bath. A solution of phenyltin trichloride (0.16 mL, 1.00 mmol) in toluene (10 mL) was added dropwise over a period of 20 min. The ice bath was removed after complete addition, and the mixture was stirred for 5 h at room temperature. The triethylammonium chloride formed was removed by filtration, and the filtrate was reduced under a vacuum. The slow evaporation of concentrated filtrate yielded crystals of pseudostannatane 3·NEt₃. Melting point: 212 °C. Yield: 49% (0.29 g, 0.49 mmol). Elemental analysis calculated for C₂₆H₃₇Cl₂NO₃Sn: C, 51.94; H, 6.20; N, 2.33. Found: C, 51.87; H, 6.16; N, 2.31. FT-IR ν (cm⁻¹): 447 (Sn–N), 502 (Sn–O), 1471 (C=C, phenyl ring), 1613 (C=C, phenyl ring), 2865, 2908, 2954 (C–H), 3395 (O–H). ¹H NMR (400 MHz, CDCl₃): 1.32 (s, 18H^{10–12,22–24}), 2.15 (s, 6H^{8,20}), 2.94 (t, 2H²⁵, ³J(¹H–¹H) = 5.4 Hz), 3.42 (t, 2H²⁶, ³J(¹H–¹H) = 5.4 Hz), 3.90 (d, 2H^{1,13}, ²J(¹H–¹H) = 12.4 Hz), 4.91 (d, 2H^{1,13}, ²J(¹H–¹H) = 12.4 Hz), 6.56 (s, 2H^{3,15}), 6.96 (s, 2H^{5,17}). ¹³C NMR (100 MHz, CDCl₃): δ (ppm) 25.6 (C^{8,20}), 30.1 (C^{10–12,22–24}), 34.5 (C^{9,21}), 46.3 (C²⁵), 56.6 (C^{1,13}), 68.1 (C²⁶), 120.1 (C^{2,14}), 129.9 (C^{5,17}), 130.4 (C^{3,15}), 130.9 (C^{4,16}), 140.2 (C^{6,18}), 151.6 (C^{7,19}). ¹¹⁹Sn NMR (149 MHz, CDCl₃): δ (ppm) –570. MS: *m/z* 414.31 [L+H]⁺, 530.18 [M–2Cl–H]⁺, 608.20 [M–2Cl+C₆H₅].

■ RESULT AND DISCUSSION

Syntheses. The tripodal ligand N(CH₂CH₂OH){CH₂(2-*t*-Bu-4-Me-C₆H₂O)}₂ (H₃L) was obtained from ethanolamine, formaldehyde, and 2-(*tert*-butyl)-4-methylphenol via the Mannich condensation reaction. The reaction of H₃L with *n*-butyltin trichloride and phenyltin trichloride in THF/Na/CH₃OH yielded aqua complexes of pseudostannatanes [LSnBu(H₂O)] (1_a) and [LSnPh(H₂O)] (2_a) as their acetone solvates 1_a·Me₂CO and 1_b·Me₂CO, respectively. However, after varying the solvent system to CH₃ONa/ethanol, the respective pseudostannatanes were obtained as their methanol complexes [LSnBu(MeOH)] (2_a) and [LSnPh(MeOH)] (2_b; see Scheme 1). In contrast, the reaction of H₃L with tin tetrachloride in THF/Et₃N yielded pseudostannatane 3 [LHSnCl₂] as a major product; however its crystals were not obtained. Interestingly, in previous attempts to synthesize pseudostannatane 2 by the reaction of H₃L and phenyltin trichloride in a toluene/Et₃N system, crystals of triethylamine solvate of [LHSnCl₂] (i.e., 3·Et₃N) were obtained instead of the formation of expected pseudostannatane [LSnPh]. The formation of the unexpected product [LHSnCl₂·NEt₃] can be justified by facile reverse Kocheshkov reactions of organochlorostannanes.^{39–44}

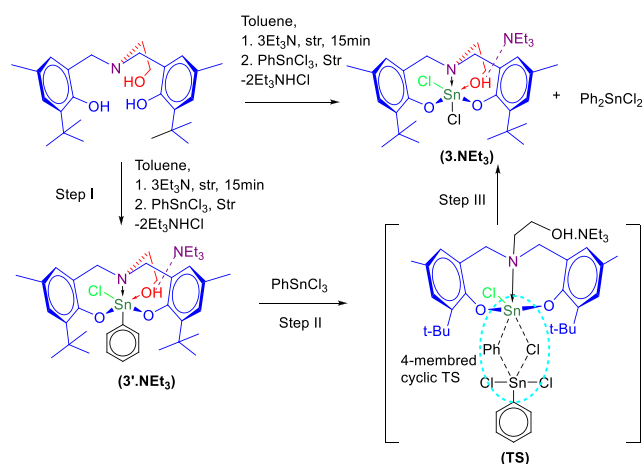
As discussed above, the reaction of H₃L with BuSnCl₃ and PhSnCl₃ in the presence of Na/MeOH yielded expected pseudostannatanes 1_a and 2_a (or 1_b/2_b in the presence of NaOMe). This is quite obvious because a strong base deprotonated H₃L at the initial stages of the reaction to form the L³⁻ anion, which coordinated the tin center to form expected products rather than a reverse Kocheshkov reaction. Moreover, reverse Kocheshkov reactions always involve the redistribution of substituents between two organochlorotin derivatives, and in the present case, all the Sn–Cl bonds are broken due to complete deprotonation of the ligand, which limits the scope of the redistribution reaction. In addition, the

theoretical calculations performed on the reaction of phenyltin trichloride and a ligand suggested the thermodynamically favorable formation of 2_b as it is an exothermic reaction and is accompanied by the release of 49.2 kcal/mol of energy. Overall, both the experimental and theoretical findings (i.e., use of strong base and exothermic reaction profile) explain why 2_b did not further undergo redistribution for the exchange of Ph and Cl groups and is isolated as a phenyl-pseudostannatane (with Ph group retained on the Sn center).

In the case of 3, the reaction of the ligand with Et₃N generated a partially deprotonated ligand HL²⁻. The partial deprotonation is observed only for the cases where Et₃N (a weak base) was used as a base and complete deprotonation was observed in the case of sodium methoxide (a strong base). It is supported by the X-ray crystallographic data of pseudostannatanes and a parallel experiment where SnCl₄ and H₃L were reacted in the presence of another strong base (NaH) to investigate the deprotonation of ligand (see section S1 in the Supporting Information). The HL²⁻ ligand coordinated a Sn atom via N, two deprotonated bisphenolic-O atoms, and a protonated ethanolic-O atom. The remaining positions were occupied by two chloro groups to form a distorted octahedral geometry. In most of the previous reports, Sn acquires hexacoordination by coordinating reactive species present in the reaction mixture or via additional reactive groups of the ligand.^{2,3} A similar trend is observed in the cases of 1_a, 1_b, 2_a, and 2_b where hexacoordination is acquired by coordinating a solvent molecule (methanol/water) in the sixth position. This type of behavior was also observed in one of our earlier reports on pseudostannatane [NEt₃][(N{CH₂(2-Me-4-Me-C₆H₂O)}₃)SnCl₂] which was isolated as an ionic product.³ In that case, despite abstraction of all three protons from the tripodal ligand (as all the arms were phenolic), Cl⁻ occupied the sixth position, resulting in the formation of triethylammonium salt of anionic pseudostannatane. However, in the formation of pseudostannatane 3, triethylamine, being a weak base, could not deprotonate the ethanolic arm. Therefore, untrapped Cl⁻ ions acted as a nucleophile and occupied one of the octahedral positions. This satisfied the covalency of Sn and eliminated the need for deprotonation of the ethanolic arm. Thus, the ethanolic arm coordinated with Sn just like the coordination of protonated solvents in the case of pseudostannatane 1 and 2. The coordination of the protonated ethanolic arm was also evidenced by the single-crystal X-ray diffraction of 3·Et₃N, which was a reverse Kocheshkov product. It had a similar structure as 3 but was isolated as triethylamine solvate due to the noncovalent interaction of triethylamine with ethanolic OH.

The phenomenon of the reverse Kocheshkov reaction and formation of 3·NEt₃ was supported by carrying DFT calculations (see Scheme 2). The molecular species involved in the reaction mechanism has been optimized by performing density functional (B3LYP/6-31G + (*d,p*)/LanL2DZ) calculations as instigated in Gaussian 09 without imposing any symmetry restrictions. The frequency calculations determined stationary points and first-order saddle points. The zero-point vibrational energy ZPVE results from the vibrational motion of molecular systems at 0 K; it was calculated as a sum of contributions from all *i* vibrational modes (harmonic oscillator model) of the molecular system. The minimum energy mechanistic route was attained for the reaction, and transition state (TS) optimization was done according to the TS Berny algorithm.⁵² The change in Gibbs free energy (ΔG) was

Scheme 2. Proposed Mechanism for Disproportionation in Phenyl Pseudostannatranes



calculated according to the equation given as $\Delta G = \Delta G_{\text{Product}} - \Delta G_{\text{Reactant}}$.

The mechanism was sketched by supposing that the reaction of H₃L and PhSnCl₃ in NEt₃/toluene should yield phenyl-pseudostannatranes (i.e., 3'.NET₃) instead of 3.NET₃ (step I). Just like 3.NET₃, it should have a deprotonated ethanolic -OH and a -Cl group (on Sn center) due to partial deprotonation of the ligand by a weak NEt₃ base. The presence of -Cl provided a means to interact with another PhSnCl₃ molecule and forms a high lying transition state (TS) which is analogous to the one documented in the literature.⁴² The transition state reported by Nechaev et al. had a four-membered cyclic transition state positioned at an energy difference of 24.8 kcal/mol from the precursor, and the energy released during the overall disproportionation reaction was reported to be 7.4 kcal/mol. In the present case, the cleavage of the coordinate bond between alcoholic oxygen and the Sn center generated a vacancy to incorporate the bond with the chloro group of PhSnCl₃. This led to the formation of a four-membered cyclic transition state constructed by two distinct Sn centers, a chloro group and a C atom of the phenyl group (see in step II). The Gibbs free energy change (ΔG -TS) for the formation of TS was found to be 46.6 kcal/mol (see Figure 1).

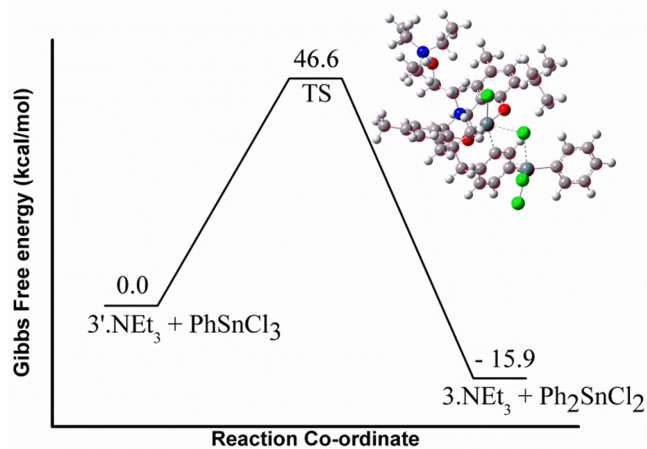


Figure 1. Energy profile for the disproportionation in the phenyl pseudostannatranes.

In step III, the four-membered cyclic transition state cleaved in such a way that the phenyl group of the stannatranes cage and the chloro group of PhSnCl₃ replaced their respective positions. Simultaneous bond formation of alcoholic oxygen and the Sn center along with ring cleavage resulted in the formation of the actual product 3.NET₃ and the byproduct Ph₂SnCl₂. The overall Gibbs free energy change for the disproportionation from 3'.NET₃ to 3.NET₃ was found to be -15.9 kcal/mol. The exothermic energy change seems to be the driving force behind the disproportionation in the reported pseudostannatranes.

The proposed mechanism was supported by monitoring the progress of the reaction spectroscopically, which evidenced the formation of 3'.NET₃ and Ph₂SnCl₂ during the reaction. For this, aliquots of the reaction mixture were taken at different time intervals (i.e., 0, 0.5, 1, 2, 3, and 4 h) and kept under an inert atmosphere at -10 °C. The ¹¹⁹Sn NMR spectrum of each aliquot was recorded in CDCl₃ and compared with the spectrum of pure PhSnCl₃ and final product (as references; Figure 2). The ¹¹⁹Sn NMR spectrum of pure PhSnCl₃ (spectrum "a") showed a signal at -62 ppm. Spectrum b, recorded for the first sample collected immediately after the addition of PhSnCl₃ to the stirred mixture of ligand and NEt₃ (time = 0 h), showed a signal of unreacted PhSnCl₃ (at -62 ppm) and a new signal at -533 ppm, suggesting the formation of new species in the reaction mixture. The signal at -533 ppm had a similar chemical shift as in the case of the 2a (-532 ppm) and the 2b (-531 ppm), suggesting the formation of phenyl pseudostannatranes (3'.NET₃). Spectrum c, recorded after half an hour of stirring, showed the appearance of two additional signals at -36 ppm and -570 ppm, which could be assigned to the Ph₂SnCl₂⁵³ and 3.NET₃, respectively. Both the signals were retained in spectra d, e, and f (recorded at 1, 2, and 3 h), confirming the presence of four tin species in the reaction mixture (i.e. PhSnCl₃, Ph₂SnCl₂, 3'.NET₃, and 3.NET₃). After 4 h (spectrum g), the signals at -62 ppm and -533 ppm disappeared owing to the complete consumption of the PhSnCl₃ and the intermediate 3'.NET₃, and signals of the final products Ph₂SnCl₂ and 3'.NET₃ remained in the reaction mixture. The ¹¹⁹Sn NMR spectroscopic study of the reaction mixture at different stages of the reaction evidenced the formation of the intermediate and its conversion into the obtained product due to the reverse Kocheshkov reaction.

Spectroscopic Studies. The FT-IR spectrum of H₃L showed vibrational bands at 3391 and 3581 cm⁻¹ due to -OH groups; however the broad vibrational bands observed in the case of pseudostannatranes 1_{a/b}, 1_b, 2_{a/b}, and 2_b at 3292, 3224, 3304, and 3201 cm⁻¹, respectively, supported the coordination of solvents. In the case of 3 and 3·Et₃N, the vibrational band corresponding to the ethanolic arm was retained at 3385 and 3395 cm⁻¹, respectively, confirming the coordination of this arm without deprotonation. The formation of the tricyclic cage was supported by the presence of the vibrational bands at 496/496, 501/504, and 501/502 cm⁻¹ due to Sn-O and at 440/441, 452/447, and 451/448 cm⁻¹ due to the Sn ← N bond for pseudostannatranes 1_{a/b}, 2_{a/b}, and 3/3·NET₃, respectively. In addition, Sn-C vibrational band in pseudostannatranes 1_{a/b} and 2_{a/b} was observed at 520/519 and 534/539 cm⁻¹, respectively.

The ¹H NMR spectrum of H₃L consisted of two triplets at 2.68 and 3.79 ppm with ³J(¹H-¹H) = 5.2 Hz due to a -CH₂CH₂- chain along with singlets at 1.38 and 2.22 ppm due to tert-butyl and methyl substituents, respectively. The signal corresponding to one hydroxyl proton appeared at 8.10

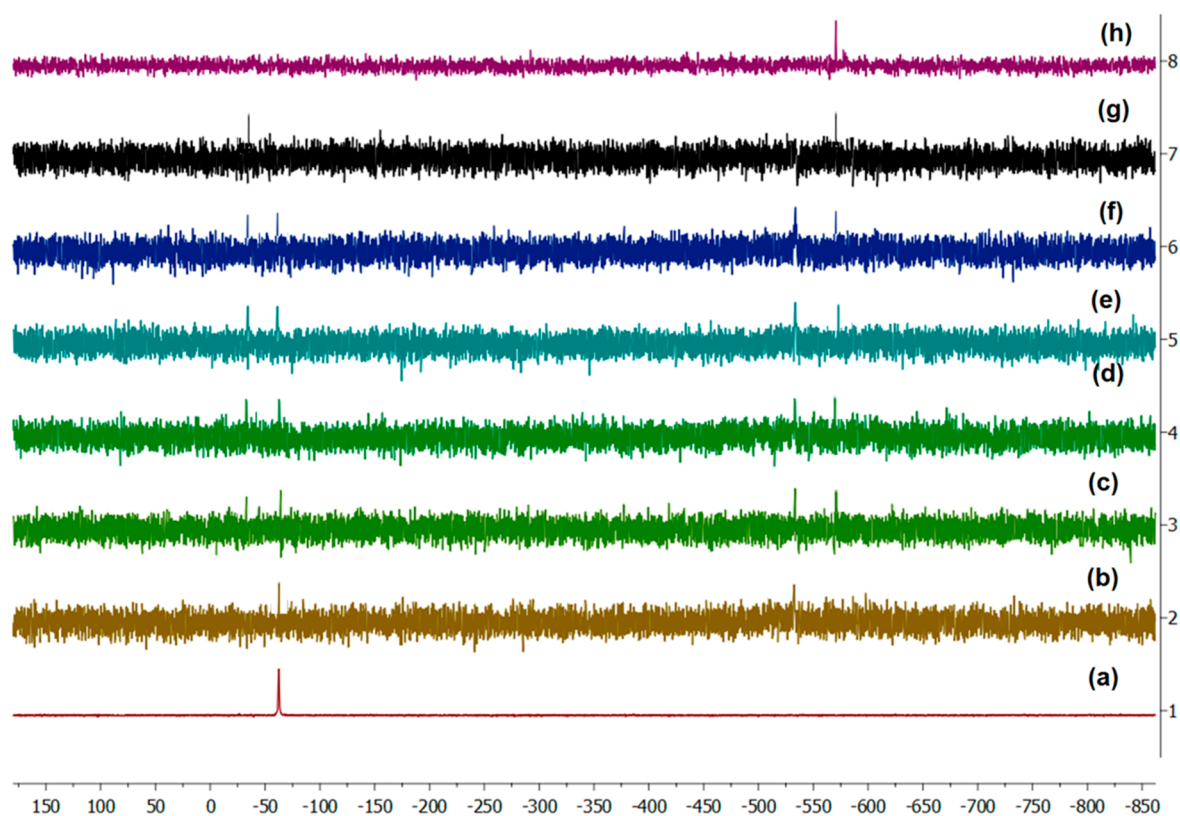


Figure 2. Comparison of ^{119}Sn NMR spectra of reaction mixture at different time intervals (in CDCl_3). (a) PhSnCl_3 as a reference, (b) 0 h, (c) 0.5 h, (d) 1 h, (e) 2 h, (f) 3 h, (g) 4 h, and (h) isolated product $3\cdot\text{NEt}_3$ as a reference.

Table 1. X-ray Crystal Data of **1–3**: Selected Bond Lengths (Å) and Angles (deg)

bond lengths [Å]	1a	1b	2a	2b	$3\cdot\text{NEt}_3^a$
Sn1–O1	2.0577(15)	2.043(2)	2.034(3)	2.030(4)	2.016(4)
Sn1–O2	2.0424(14)	2.057(2)	2.035(3)	2.116(3)	2.031(4)
Sn1–O3	2.0429(15)	2.334(3)	2.043(3)	2.444(3)	2.046(4)
Sn1–O4	2.2802(15)	2.032(2)	2.262(4)	2.080(3)	
Sn1–N1	2.2730(18)	2.271(3)	2.266(4)	2.207(4)	2.266(5)
Sn1–C27	2.125(2)	2.121(4)	2.135(5)	2.002(3)	
	bond angles (deg)				
O1–Sn1–O4	81.51(6)	98.71(10)	171.84(12)	154.18(15)	
O1–Sn1–O2	96.46(6)	95.99(10)	98.74(13)	95.24(13)	92.54(18)
O1–Sn1–O3	157.60(7)	170.86(9)	95.06(14)	82.11(13)	166.84(18)
O2–Sn1–O3	98.21(6)	80.00(10)	158.91(14)	171.10(12)	94.00(18)
O2–Sn1–O4	171.00(6)	157.64(11)	83.06(14)	105.47(13)	-
O3–Sn1–O4	81.36(6)	82.92(10)	81.13(15)	75.06(13)	-
O1–Sn1–N1	79.13(6)	86.81(9)	87.29(13)	85.12(15)	88.08(18)
O2–Sn1–N1	86.46(6)	79.12(10)	84.74(13)	92.62(13)	86.97(16)
O3–Sn1–N1	84.97(6)	84.37(10)	80.06(14)	78.71(13)	80.89(16)
O4–Sn1–N1	84.55(6)	84.95(9)	84.95(14)	78.79(14)	
C27–Sn1–N1	174.78(8)	172.85(14)	174.33(15)	171.30(14)	

^aSome additional parameters of $3\cdot\text{NEt}_3$. Bond lengths: Sn1–Cl1, 2.4822(16); Sn1–Cl2, 2.3619(17); Bond angles: Cl2–Sn1–Cl1, 90.38(7); O1–Sn1–Cl1, 87.24(13); O1–Sn1–Cl2, 93.73(15); O2–Sn1–Cl1, 178.36(13); O2–Sn1–Cl2, 91.26(12); O3–Sn1–Cl1, 85.89(13); O3–Sn1–Cl2, 97.52(13); N1–Sn1–Cl1, 91.39(12); N1–Sn1–Cl2, 177.53(13)

ppm as a broad signal. The ^1H NMR data of pseudostannatranes **1_a** and **2_a** were found almost similar to **1_b** and **2_b**; therefore the data discussed below correspond to **1_a** and **2_a**. The formation of pseudostannatranes **1_a** was confirmed by the appearance of signals in the region 0.92–1.87 ppm due to the n-butyl group in addition to the signals of the ligating skeleton. The diastereotopic protons at positions 1 and 13 appeared as

doublets at 3.60 and 4.31 ppm due to geminal coupling (with $^2J(^1\text{H}-^1\text{H}) = 12.0$ Hz). Similarly, the formation of pseudostannatranes **2_a** was confirmed by the appearance of additional signals in the aromatic region, i.e., a multiplet within 7.31–7.97 ppm and a doublet at 7.97 ppm due to the phenyl substituent. The binding of phenyl with a Sn atom was observed as satellites around the $\text{H}^{28,32}$ doublet with

$^3J(^1\text{H}-^{117}\text{Sn}) = 85.6$ Hz and $^3J(^1\text{H}-^{119}\text{Sn}) = 98.4$ Hz. The ^1H NMR of pseudostannatranes **3** consisted of the signals of the ligating cage. It was not isolated in crystalline form (obtained as a powder); however, the signals of the major product correspond to NMR signals of pseudostannatranes **3**·NEt₃. The spectrum of pseudostannatranes **3**·NEt₃ had all the signals of the ligating skeleton including two doublets due to diastereotopic protons, which indicated the coordination of the ligating system with Sn (as these signals appear as a singlet in free ligand).

The ^{13}C NMR of pseudostannatranes showed characteristic signals of all carbon atoms with the signals corresponding to *n*-butyl groups in the region 13.6–27.4 ppm and to phenyl in the regions 126.9–136.2 ppm and 127.0–136.2 ppm for **1**_{a/b} and **2**_{a/b}, respectively. The ^{119}Sn NMR signal of pseudostannatranes **1**_{a/b} and **2**_{a/b} appeared at –476/–477 and –532/–531 ppm, respectively. The pseudostannatranes **3**·NEt₃ showed a signal at –570 ppm, whereas the spectrum of pseudostannatranes **3** consisted of four signals at –565, –569, –625, and –669 ppm, suggesting the formation of multiple species in the solution phase. The mass spectra of pseudostannatranes **1**_{a/b} and **2**_{a/b} exhibited molecular ion peaks at *m/z* 588.26/588.20 and 608.23/608.20, respectively, along with the fragmentation peak due to the ligand at *m/z* 414.31. In contrast, **3**/3·NEt₃ exhibited a peak at *m/z* 530.18 which corresponded to the [LSn] fragment formed after the loss of the two chloride ions.

Single Crystal X-ray Diffraction Studies. All the pseudostannatranes were obtained in crystalline forms (except **3**), and their structures were elucidated by X-ray crystallography. Selected bond lengths and bond angles for pseudostannatranes **1**_{a,b}, **2**_{a,b}, and **3**·NEt₃ are presented in Table 1 and their crystallographic data and structure refinement parameters are listed in Table S1 (see caption of Figure 3 for selected bond lengths and bond angles of ligand).

The ligand H₃L was crystallized in the *Pbca* space group of the orthorhombic crystal system. Some intramolecular hydrogen bond contacts were found between O3–H3···N1 (2.011 Å) and O2–H2···O1B (2.063 Å; shown in Figure 3). Although the solid-state structure of H₃L is in agreement with the ^1H

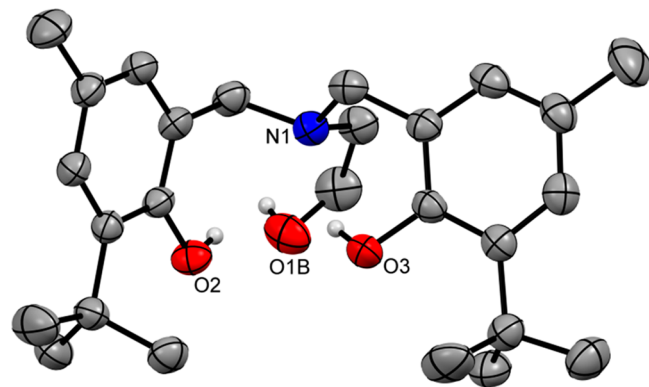


Figure 3. ORTEP presentation of H₃L with the partial numbering scheme (thermal ellipsoids were drawn at 30% probability and hydrogen atoms have been omitted for clarity). [Some bond lengths (in Å): O1A–C1A, 1.390(20); O1B–C1B, 1.465(18); O2–C9, 1.372(2); O3–C21, 1.367(3); N1–C3, 1.477(3); N1–C2, 1.486(3); N1–C15, 1.464(3). Bond angles (in deg): C3–N1–C2, 110.1(2); C2–N1–C15, 112.3(2); C3–N1–C15, 111.3(2); O1A–C1A–C2, 115.3(12); O1B–C1B–C2, 107.0(10); O2–C9–C4, 119.9(2); O2–C9–C8, 118.6(2).]

and ^{13}C NMR investigation, the hydrogen bond interactions observed in the solid-state structure, however, were absent in the solution phase permitting the free rotation of arms. Therefore, methylene protons H¹ and H¹³ appeared as a singlet that is otherwise restrictive based on crystal structure and would have led to diastereotopic protons as seen in the case of pseudostannatranes. The free rotation of these arms also led to some disorders in its solid-state structure. The ethanolic arm was found to be split, and as a consequence, an alcoholic –OH did not find any acceptor for hydrogen bonding. This type of disorder and important structural parameters (bond lengths and bond angles) of H₃L are consistent with the reported structures of the related ligand.³⁸

The mononuclear pseudostannatranes **1**_a was crystallized as an acetone solvate **1**_a·Me₂CO in the triclinic crystal system with the *P1* space group. The crystal structure showed a [4.4.3.0^{1,5}]tridecane cage with distorted octahedral geometry around Sn (Figure 4). The coordination sphere of Sn consisted

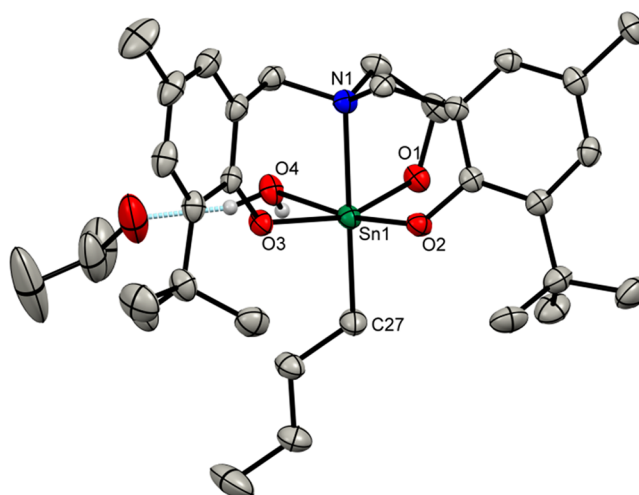


Figure 4. ORTEP presentation of **1**_a·Me₂CO with the partial numbering scheme (thermal ellipsoids were drawn at 30% probability, and hydrogen atoms have been omitted for clarity).

of three oxygen atoms of the tripodal tetradentate ligand and a water molecule at a square planar position. The water molecule could have arrived from the moisture in the air during the crystallization process.

The remaining sites were occupied by a nitrogen atom and *n*-butyl chain. The water molecule was further bonded to the acetone molecule via noncovalent interactions and stabilized the crystal lattice. Despite the unsymmetrical podands and different *trans* substituents, the three Sn–O bonds formed by L³⁻ were essentially similar (Sn1–O1, 2.0577(15); Sn1–O2, 2.0424(14); Sn1–O3, 2.0429(15) Å). The Sn1–O4 (2.2802(15) Å) bond length was found to be different from the rest as it originated from the coordinated water molecule. The Sn–C and transannular Sn–N bond lengths were found to be 2.125(2) and 2.2730(18), respectively. The sum of the equatorial O–Sn–O angles is 357.5(2)°, and the Sn atom occupied a position slightly out of the plane toward the exocyclic *n*-butyl group.

Pseudostannatranes **1**_b was also crystallized in the triclinic crystal system with the *P1* space group. Its structural features were similar to **1**_a except for the coordination of methanol with the Sn instead of a water molecule. The sum of the equatorial

O–Sn–O angles is $357.6(4)^\circ$, and the Sn atom was seen slightly tilted toward the *n*-butyl group (Figure 5). The three

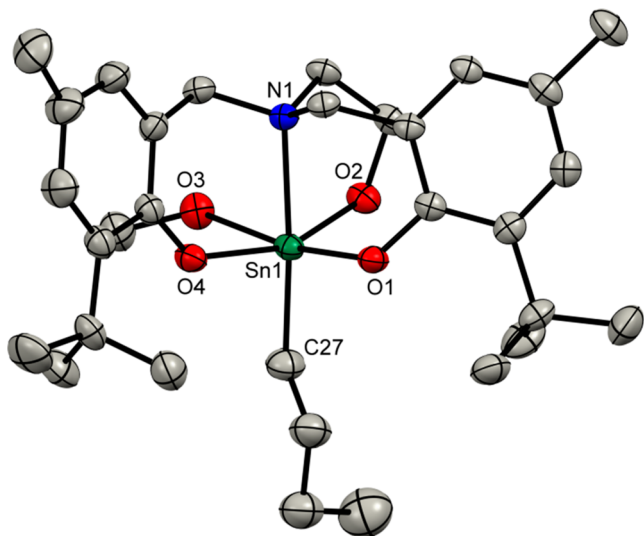


Figure 5. ORTEP presentation of **1_b** with the partial numbering scheme (thermal ellipsoids were drawn at 30% probability and hydrogen atoms have been omitted for clarity).

Sn–O bond lengths originating from the ligand coordination are comparable (Sn1–O1:2.043(2), Sn1–O2:2.057(2), and Sn1–O4:2.032(2) Å), whereas Sn1–O3 was found to be slightly longer (i.e., 2.334(3) Å). The Sn–C and transannular Sn–N bond lengths were found to be the same as in **1_a**.

The pseudostannatranes **2_a** was crystallized as its acetone solvate **2_a·Me₂CO** in the $P\bar{1}$ space group of the triclinic system. It consisted of a similar cage to that of **1_a** and **1_b** with octahedral geometry around the tin. The tripodal tetradentate cage occupied three equatorial and an axial position, while the phenyl ring and water occupied the rest of the positions (Figure 6). The sum of all the equatorial angles was found to be $358.0(6)^\circ$ with comparable Sn–O bond lengths.

Unlike the other pseudostannatranes, **2_b** was crystallized in the $P2_1/n$ space group of the monoclinic crystal system (Figure 7). Its structure was the same as **2_a**, however, it involved a

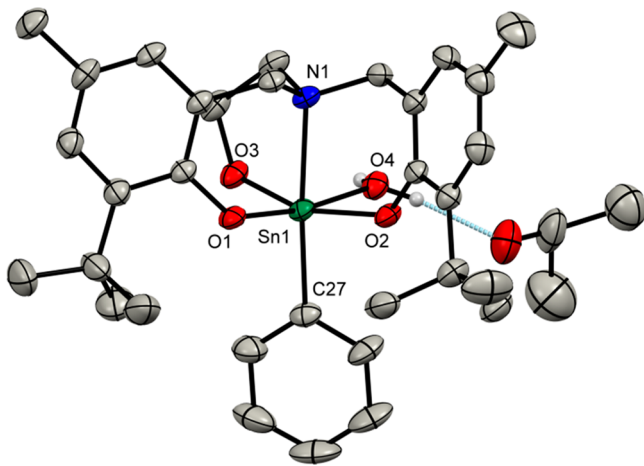


Figure 6. ORTEP presentation of **2_a·Me₂CO** with the partial numbering scheme (thermal ellipsoids were drawn at the 30% probability, and hydrogen atoms have been omitted for clarity).

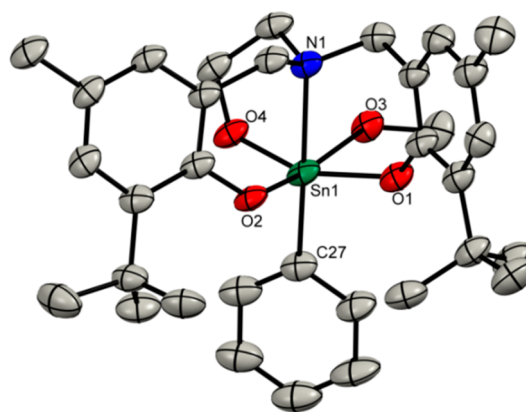


Figure 7. ORTEP presentation of **2_b** with the partial numbering scheme (thermal ellipsoids were drawn at 30% probability and hydrogen atoms have been omitted for clarity).

direct bond between Sn and methanol (instead of water) at the equatorial position. The deviation of octahedral geometry was confirmed by the sum of all the equatorial bond angles equal to $357.9(5)^\circ$.

Single-crystal X-ray diffraction analysis of **3·NEt₃** revealed the formation of a [4.4.3.0^{1,5}]tridecane cage, which was cocrystallized with a triethylamine molecule (Figure 8).

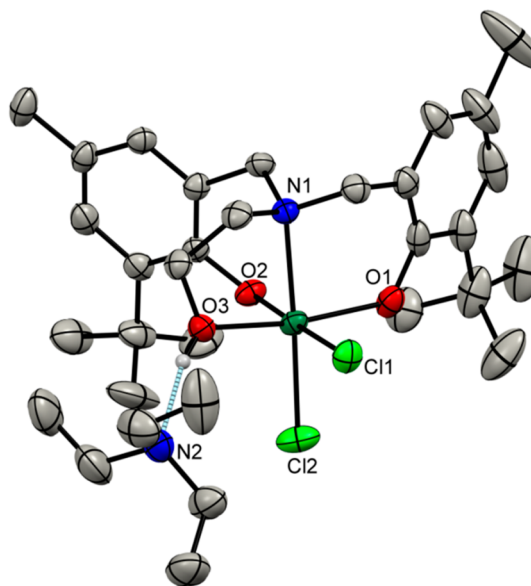


Figure 8. ORTEP presentation of **3·NEt₃** with the partial numbering scheme (thermal ellipsoids were drawn at 30% probability, whereas hydrogen atoms have been omitted for clarity).

It featured hexacoordinated Sn in which the ligand was coordinated in such a way that its N atom and one of the oxygen atoms are situated *trans* to the Cl groups. Despite the different *trans* donors, the three Sn–O bond lengths were found to be practically the same (Sn–O1 2.016(4), Sn–O2 2.031(4), and Sn–O3 2.046(4) Å). The Sn–Cl bond lengths were more responsive to their distinct *trans*-donor environment and are found to be Sn–Cl1 = 2.4822(16) and Sn–Cl2 = 2.3619(17) Å.

All of the six-membered fused rings in pseudostannatranes **1–3** assumed twist-boat conformations, whereas the five-membered fused rings acquired a uniform enveloped

conformation and made the molecules chiral in terms of Δ and Λ stereochemistry. Pseudostannatranes $1_{a/b}$ and $2_{a/b}$ each contained only one crystallographically independent molecule but as a pair of enantiomers in their unit cell, $\Delta/\Lambda-1_a$, $\Delta/\Lambda-1_b$, $\Delta/\Lambda-2_a$, and $\Delta/\Lambda-2_b$, whereas the unit cell of pseudostannatranes $3\cdot\text{NEt}_3$ consisted of only one crystallographically independent molecule with clockwise ($\Delta-3\cdot\text{NEt}_3$) orientation of the propellers when viewed along the Z–Sn–N axis. All of the pseudostannatranes cages showed distorted octahedral geometry. One of the efficient criteria of the “goodness” of the octahedral geometry is the difference ($\Delta\sum(\theta)^\circ$) of equatorial and axial angles, which is 0° ($4 \times 90^\circ$ to $4 \times 90^\circ$) for the ideal octahedron.^{15,54} The geometric goodness $\Delta\sum(\theta)^\circ$ of the octahedral configuration of the tin atoms in pseudostannatranes 1–3 lies in the range between 13.22° and 26.22° and depicts a strong distortion from the ideal geometry (Table 2). In pseudostannatranes $1_{a/b}$ and $2_{a/b}$

Table 2. Geometrical Goodness of the Octahedral Geometry $\Delta\sum(\theta)^\circ$ and Distances $\Delta(E(\text{O}_{\text{eq}}/\text{Cl}_{\text{eq}})-\text{Sn})$ for Pseudostannatranes $1_{a/b}$, $2_{a/b}$, and $3\cdot\text{NEt}_3$

pseudostannatranes	$ \Delta\sum(\theta)^\circ $ (deg)	$\Delta(E(\text{O}_{\text{eq}}/\text{Cl}_{\text{eq}})-\text{Sn})$ (Å)
1a	26.22	0.222
1b	25.02	0.220
2a	23.51	0.202
2b	24.63	0.207
$3\cdot\text{NEt}_3$	13.22	0.116

the equatorial positions were occupied by O1–O4, whereas they were taken up by O1–O3 and Cl1 in pseudostannatranes $3\cdot\text{NEt}_3$. The displacement of the tin atom was found to be in the direction of the exocyclic ligand from the mean equatorial plane $E(\text{O}_{\text{eq}}/\text{Cl}_{\text{eq}})$ of oxygen/chlorine atoms (Table 2).

CONCLUSION

The pseudostannatranes 1–3 were obtained as mononuclear entities with hexacoordination at the Sn atom. The ligating system possessing bulky substituents certainly disfavored the formation of oligomeric tin(IV) compounds for which the oligomerization is pretty much common possibly due to weaker steric constraints. The formation of the octahedral tin coordination sphere is assisted by the coordination of solvent in the case of pseudostannatranes 1_a , 1_b , 2_a , and 2_b and monodentate Cl^- ligands in the case of 3 and $3\cdot\text{Et}_3\text{N}$. The partial deprotonation of the ligand resulted in the retention of the Sn–Cl bond, which provides a means for the reverse Kocheshkov reaction and yielded a different product $3\cdot\text{Et}_3\text{N}$ instead of 2. The partial deprotonation is observed only for the cases where Et_3N (a weak base) was used as a base and complete deprotonation was observed in the case of sodium methoxide (a strong base). The experimental findings have been rationalized by exhaustive density functional calculations that provide conclusive evidence for the results presented in the study.

ASSOCIATED CONTENT

Supporting Information

The Supporting Information is available free of charge at <https://pubs.acs.org/doi/10.1021/acs.inorgchem.0c01202>.

FT-IR spectra; ^1H , ^{13}C , ^{119}Sn spectra; ESI-MS spectra; optimized geometry of transition state; and the table

containing crystallographic data and structure refinement parameters (PDF)

Accession Codes

CCDC 1950219 (H_3L), 1950224 (1_a), 1950229 (1_b), 1950240 (2_a), 1950241 (2_b) and 1950262 ($3\cdot\text{NEt}_3$) contain the supplementary crystallographic data for this paper. These data can be obtained free of charge via www.ccdc.cam.ac.uk/data_request/cif, or by emailing data_request@ccdc.cam.ac.uk, or by contacting The Cambridge Crystallographic Data Centre, 12 Union Road, Cambridge CB2 1EZ, UK; fax: + 44 1223 336033.

AUTHOR INFORMATION

Corresponding Authors

Raghubir Singh – Department of Chemistry, DAV College, Chandigarh 160011, India; Email: raghu_chem2006@yahoo.com

Varinder Kaur – Department of Chemistry, Panjab University, Chandigarh 160014, India; orcid.org/0000-0002-4585-0426; Email: var_ka04@yahoo.co.in, var_ka04@pu.ac.in

Authors

Keshav Kumar – Department of Chemistry, Panjab University, Chandigarh 160014, India; orcid.org/0000-0001-7001-0034

Neha Srivastav – Department of Chemistry, Panjab University, Chandigarh 160014, India

Mayank Khara – Department of Chemistry, Panjab University, Chandigarh 160014, India

Neetu Goel – Department of Chemistry, Panjab University, Chandigarh 160014, India; orcid.org/0000-0001-5345-0783

Complete contact information is available at: <https://pubs.acs.org/doi/10.1021/acs.inorgchem.0c01202>

Notes

The authors declare no competing financial interest.

ACKNOWLEDGMENTS

The authors are thankful to DST, New Delhi [EMR/2016/006530] for providing financial support. Dr. Raghubir Singh and Dr. Varinder Kaur dedicate this work to Dr. Jörg Wagler, Institut für Anorganische Chemie, Technische Universität Bergakademie, Freiberg–09596 Freiberg, Germany for his continuous support.

REFERENCES

- Simidzija, P.; Lecours, M. J.; Marta, R. A.; Steinmetz, V.; McMahon, T. B.; Fillion, E.; Hopkins, W. S. Changes in Tricarbostannatranes Transannular N–Sn Bonding upon Complexation Reveal Lewis Base Donicities. *Inorg. Chem.* **2016**, *55*, 9579–9585.
- Srivastav, N.; Kumar, K.; Singh, R.; Kaur, V. Tricyclic Tin(IV) Cages: Synthetic Aspects and Intriguing Features of Stannatranes and Pseudostannatranes. *New J. Chem.* **2020**, *44*, 3168–3184.
- Srivastav, N.; Singh, R.; Kaur, V.; Wagler, J.; Kroke, E. A Stannatranes-like [4.4.4.0^{1,6}] Heterotricyclic Stannate Anion Possessing Rhodanide Antennae: A Chromoreactand for Fe^{3+} , Cu^{2+} and Co^{2+} Ions. *Inorg. Chim. Acta* **2017**, *463*, 54–60.
- Srivastav, N.; Mutneja, R.; Singh, N.; Singh, R.; Kaur, V.; Wagler, J.; Kroke, E. Diverse Molecular Architectures of Si and Sn [4.4.3.0^{1,6}] Tridecane Cages Derived from a Mannich Base Possessing Semi-Rigid Unsymmetrical Podands. *Eur. J. Inorg. Chem.* **2016**, *2016*, 1730–1737.

- (5) Singh, N.; Kumar, K.; Srivastav, N.; Singh, R.; Kaur, V.; Jasinski, J. P.; Butcher, R. J. Exploration of Fluorescent Organotin Compounds of α -Amino Acid Schiff Bases for the Detection of Organophosphorous Chemical Warfare Agents: Quantification of Diethylchlorophosphate. *New J. Chem.* **2018**, *42*, 8756–8764.
- (6) Glowacki, B.; Lutter, M.; Alnasr, H.; Seymen, R.; Hiller, W.; Jurkschat, K. Introducing Stereogenic Centers to Group XIV Metallatrane. *Inorg. Chem.* **2017**, *56*, 4937–4949.
- (7) Glowacki, B.; Lutter, M.; Hiller, W.; Jurkschat, K. Control of λ -And Δ -Isomerization of the Atrane Cages in Group XIV Metallatrane by Chiral Axial Substituents. *Inorg. Chem.* **2019**, *58*, 4244–4252.
- (8) Glowacki, B.; Lutter, M.; Schollmeyer, D.; Hiller, W.; Jurkschat, K. Novel Stannatranes $N(CH_2CMe_2O)_2(CMe_2CH_2O)SnO$ -t-Bu and Related Oligonuclear Tin(IV) Oxoclusters. Two Isomers in One Crystal. *Inorg. Chem.* **2016**, *55*, 10218–10228.
- (9) Voronkov, M. G.; Baryshok, V. P. Metallatrane. *J. Organomet. Chem.* **1982**, *239*, 199–249.
- (10) Verkade, J. G. Atranes: New Examples with Unexpected Properties. *Acc. Chem. Res.* **1993**, *26*, 483–489.
- (11) Verkade, J. G. Main Group Atranes: Chemical and Structural Features. *Coord. Chem. Rev.* **1994**, *137*, 233–295.
- (12) Karlov, S. S.; Tyurin, D. A.; Zabalov, M. V.; Churakov, A. V.; Zaitseva, G. S. Quantum Chemical Study of Group 14 Elements Pentacoordinated Derivatives - Metallatrane. *J. Mol. Struct.: THEOCHEM* **2005**, *724*, 31–37.
- (13) Martinez, A.; Robert, V.; Gornitzka, H.; Dutasta, J. P. Controlling Helical Chirality in Atrane Structures: Solvent-Dependent Chirality Sense in Hemicryptophane-Oxidovanadium(V) Complexes. *Chem. - Eur. J.* **2010**, *16*, 520–527.
- (14) Tasaka, M.; Hirotsu, M.; Kojima, M.; Utsuno, S.; Yoshikawa, Y. Syntheses, Characterization, and Molecular Mechanics Calculations of Optically Active Silatrane Derivatives. *Inorg. Chem.* **1996**, *35*, 6981–6986.
- (15) Zöllner, T.; Dietz, C.; Iovkova-Berends, L.; Karsten, O.; Bradtmöller, G.; Wiegand, A.-K.; Wang, Y.; Jouikov, V.; Jurkschat, K. Novel Stannatranes of the Type $N(CH_2CMe_2O)_3SnX$ ($X = OR, SR, OC(O)R, SP(S)Ph_2, Halogen$). Synthesis, Molecular Structures, and Electrochemical Properties. *Inorg. Chem.* **2012**, *51*, 1041–1056.
- (16) Zöllner, T.; Jurkschat, K. Novel Trialkanolamine Derivatives of Tin of the Type $[N(CH_2CMe_2O)_2(CH_2)_nOSnOR]_m$ ($m = 1, 2; n = 2, 3; R = t\text{-Bu}, 2,6\text{-Me}_2C_6H_3$) and Related Tri- and Pentanuclear Tin(IV) Oxoclusters. Syntheses and Molecular Structures. *Inorg. Chem.* **2013**, *52*, 1872–1882.
- (17) Jurkschat, K.; Mügge, C.; Tzschach, A.; Zschunke, A.; Engelhardt, G.; Lippmaa, E.; Mägi, M.; Larin, M. F.; Pestunovich, V. A.; Voronkov, M. G. $^1H, ^{13}C, ^{15}N$ and ^{119}Sn NMR Investigations on Stannatranes. *J. Organomet. Chem.* **1979**, *171*, 301–308.
- (18) Jurkschat, K.; Tzschach, A. 1-Aza-5-Stanna-5,5-Dimethylbicyclo[3.3.0 1,5] Octan Und 1-Aza-5-Stanna-5-Methyltricyclo[3.3.3.0 1,5] Undecan, Pentakoordinierte Tetraorganozinnverbindungen. *J. Organomet. Chem.* **1984**, *272*, C13–C16.
- (19) Jurkschat, K.; Tzschach, A.; Meunier-Piret, J. Crystal and Molecular Structure of 1-Aza-5-Stanna-5-Methyltricyclo[3.3.3.0 1,5]-Undecane. Evidence for a Transannular Donor–acceptor Interaction in a Tetraorganotin Compound. *J. Organomet. Chem.* **1986**, *315*, 45–49.
- (20) Jurkschat, K.; Tzschach, A.; Meunier-Piret, J.; Van Meerssche, M. Crystal and Molecular Structure of 1-Aza-5-Stanna-5-Chlorotricyclo[3.3.3.0 1,5]Undecane, a 2,8,9-Tricarbastannatranes. *J. Organomet. Chem.* **1985**, *290*, 285–289.
- (21) Kavooosi, A.; Fillion, E. Synthesis and Characterization of Tricarbastannatranes and Their Reactivity in $B(C_6F_5)_3$ -Promoted Conjugate Additions. *Angew. Chem., Int. Ed.* **2015**, *54*, 5488–5492.
- (22) Yang, C.; Jensen, M. S.; Conlon, D. A.; Yasuda, N.; Hughes, D. L. A Simple and Scalable Method to Prepare 1-Aza-5-Chloro-5-Stannabicyclo[3.3.3]Undecane. *Tetrahedron Lett.* **2000**, *41*, 8677–8681.
- (23) Yasuda, N. Application of Cross-Coupling Reactions in Merck. *J. Organomet. Chem.* **2002**, *653*, 279–287.
- (24) Wang, C.-Y.; Derosa, J.; Biscoe, M. R. Configurationally Stable, Enantioenriched Organometallic Nucleophiles in Stereospecific Pd-Catalyzed Cross-Coupling Reactions: An Alternative Approach to Asymmetric Synthesis. *Chem. Sci.* **2015**, *6*, 5105–5113.
- (25) Vedejs, E.; Haight, A. R.; Moss, W. O. Internal Coordination at Tin Promotes Selective Alkyl Transfer in the Stille Coupling Reaction. *J. Am. Chem. Soc.* **1992**, *114*, 6556–6558.
- (26) Li, L.; Wang, C.-Y.; Huang, R.; Biscoe, M. R. Stereoretentive Pd-Catalyzed Stille Cross-Coupling Reactions of Secondary Alkyl Azastannatranes and Aryl Halides. *Nat. Chem.* **2013**, *5*, 607–612.
- (27) Jensen, M. S.; Yang, C.; Hsiao, Y.; Rivera, N.; Wells, K. M.; Chung, J. Y. L.; Yasuda, N.; Hughes, D. L.; Reider, P. J. Synthesis of an Anti-Methicillin-Resistant Staphylococcus Aureus (MRSA) Carbapenem via Stannatranes-Mediated Stille Coupling. *Org. Lett.* **2000**, *2*, 1081–1083.
- (28) Dakternieks, D.; Dyson, G.; Jurkschat, K.; Tozer, R.; Tiekink, E. R. T. Utilization of Hypervalently Activated Organotin Compounds in Synthesis. Preparation and Reactions of $Me_2N(CH_2)_3SnPh_3$. *J. Organomet. Chem.* **1993**, *458*, 29–38.
- (29) Zöllner, T.; Jurkschat, K. Novel Trialkanolamine Derivatives of Tin of the Type $[N(CH_2CMe_2O)_2(CH_2)_nOSnOR]_m$ ($m = 1, 2; n = 2, 3; R = t\text{-Bu}, 2,6\text{-Me}_2C_6H_3$) and Related Tri- and Pentanuclear Tin(IV) Oxoclusters. Syntheses and Molecular Structures. *Inorg. Chem.* **2013**, *52*, 1872–1882.
- (30) Garrido, M. D.; García-Llacer, C.; El Haskouri, J.; Marcos, M. D.; Sánchez-Royo, J. F.; Beltrán, A.; Amorós, P. Atrane Complexes Chemistry as a Tool for Obtaining Trimodal UVM-7-like Porous Silica. *J. Coord. Chem.* **2018**, *71*, 776–785.
- (31) Hostettler, F.; Cox, E. F. Organotin Compounds in Isocyanate Reactions. Catalysts for Urethane Technology. *Ind. Eng. Chem.* **1960**, *52*, 609–610.
- (32) Liu, W.; Cao, J.; Fan, C.; Chen, Z. Synthesis and Catalytic Property of V-MCM-41 Mesoporous Molecular Sieves by Atrane Route. *Adv. Mater. Res.* **2011**, *284*, 936–939.
- (33) Nomura, K.; Tewasekson, U.; Takii, Y. Synthesis of Titanium Complexes Containing an Amine Triphenolate Ligand of the Type $[TiX\{(O-2,4-R_2C_6H_2)-6-CH_2\}_3N]$ and the Ti-Al Heterobimetallic Complexes with $AlMe_3$: Effect of a Terminal Donor Ligand in Ethylene Polymerization. *Organometallics* **2015**, *34*, 3272–3781.
- (34) Silva, A. L.; Bordado, J. C. Recent Developments in Polyurethane Catalysis: Catalytic Mechanisms Review. *Catal. Rev.: Sci. Eng.* **2004**, *46*, 31–51.
- (35) Tan, X. W.; Wang, B. M.; Wang, Y.; Zhan, S. Z. Design, Synthesis, Structure and Magnetic Behavior of a High Spin Binuclear Fe(III) Complex of N-(1-Ethanol)-N,N-Bis(3-Tert-Butyl-5-Methyl-2-Hydroxybenzyl) Amine. *Inorg. Chem. Commun.* **2010**, *13*, 1061–1063.
- (36) Tan, X. W.; Chen, J. Y.; Xie, X. H.; Zhan, S. Z.; Deng, Y. F. Synthesis, Structure, and Properties of a Binuclear Fe(III) Complex with N-(1-Propanol)-N,N-Bis(3-Tert-Butyl-5-Methyl-2-Hydroxybenzyl) Amine. *Transition Met. Chem.* **2010**, *35*, 999–1003.
- (37) Wichmann, O.; Sopo, H.; Lehtonen, A.; Sillanpää, R. Oxidovanadium(V) Complexes with Aminoethanol Bis(Phenolate) $[O,N,O,O']$ Ligands: Preparations, Structures, N-Dealkylation and Condensation Reactions. *Eur. J. Inorg. Chem.* **2011**, *2011*, 1283–1291.
- (38) Dean, R. K.; Fowler, C. L.; Hasan, K.; Kerman, K.; Kwong, P.; Trudel, S.; Leznoff, D. B.; Kraatz, H. B.; Dawe, L. N.; Kozak, C. N. Magnetic, electrochemical and spectroscopic properties of iron(III) amine–bis(phenolate) halide complexes. *Dalton Trans.* **2012**, *41*, 4806–4816.
- (39) Vollano, J. F.; Day, R. O.; Holmes, R. R. Pentacoordinated Molecules. 55. New Five-Coordinated Anionic Tin(IV) Complexes. Synthesis and Molecular Structure of Halodimethylstannoles Containing Rings with Mixed Ligands. *Organometallics* **1984**, *3*, 750–755.
- (40) Thoonen, S. H. L.; van Hoek, H.; de Wolf, E.; Lutz, M.; Spek, A. L.; Deelman, B.-J.; van Koten, G. Synthesis of Novel Terdentate N,C,N'-Coordinated Butyltin(IV) Complexes and Their Redistribution Reactions with $SnCl_4$. *J. Organomet. Chem.* **2006**, *691*, 1544–1553.

(41) Portnyagin, I. A.; Nechaev, M. S.; Khrustalev, V. N.; Zemlyansky, N. N.; Borisova, I. V.; Antipin, M. Y.; Ustynyuk, Y. A.; Lunin, V. V. An Unusual Reaction of (β -Dimethylaminoethoxy)-Triethyltin with Phenyltin Trichloride. The First X-Ray Structural Evidence of the Existence of Complexes $R_2SnXY \cdot R_2SnXY$ (R = Alkyl, Aryl; X, Y = Hal, OR, X \neq Y) Both as Unsymmetrical Adducts [$R_2SnX_2 \cdot R_2SnY_2$] *An. Eur. J. Inorg. Chem.* **2006**, 2006, 4271–4277.

(42) Portnyagin, I. A.; Lunin, V. V.; Nechaev, M. S. Reverse Kocheshkov Reaction – Redistribution Reactions between $RSn(OCH_2CH_2NMe_2)_2Cl$ (R = Alk, Ar) and $PhSnCl_3$: Experimental and DFT Study. *J. Organomet. Chem.* **2008**, 693, 3847–3850.

(43) Nguyen Van, D.; Lindberg, R.; Frech, W. Redistribution Reactions of Butyl- and Phenyltin Species during Storage in Methanol. *J. Anal. At. Spectrom.* **2005**, 20, 266.

(44) Airapetyan, D. V.; Petrosyan, V. S.; Gruener, S. V.; Zaitsev, K. V.; Arkhipov, D. E.; Korlyukov, A. A. Disproportionation Reactions within the Series of Coordinated Monoorganostannanes. *J. Organomet. Chem.* **2013**, 747, 241–248.

(45) Dolomanov, O. V.; Bourhis, L. J.; Gildea, R. J.; Howard, J. A. K.; Puschmann, H. OLEX2: A Complete Structure Solution Refinement and Analysis Program. *J. Appl. Cryst.* **2009**, 42, 339–341, DOI: 10.1107/S0021889808042726.

(46) Sheldrick, G. M. Crystal Structure Refinement with SHELXL. *Acta Crystallographica Section C* **2014**, C71, 3–8, DOI: 10.1107/S2053229614024218.

(47) Sheldrick, G. M. Research Papers SHELXT Integrated Space-Group and Crystal-Structure Determination Research Papers. *Acta Crystallographica Section A* **2014**, A71, 3–8, DOI: 10.1107/S2053273314026370.

(48) Becke, A. D. Density-Functional Thermochemistry. III. *J. Chem. Phys.* **1993**, 98, 5648–5652.

(49) Lee, C.; Hill, C.; Carolina, N. *Into a Functional of the Electron Density f F* **1988**, 37, 785–789.

(50) Frisch, M. J.; Trucks, G. W.; Schlegel, H. B.; Scuseria, G. E.; Robb, M. A.; Cheeseman, J. R.; Scalmani, G.; Barone, V.; Petersson, G. A.; Nakatsuji, H.; Li, X.; Caricato, M.; Marenich, A.; Bloino, J.; Janesko, B. G.; Gomperts, R.; Mennucci, B.; Hratchian, H. P.; Ortiz, J. V.; Izmaylov, A. F.; Sonnenberg, J. L.; Williams-Young, D.; Ding, F.; Lipparini, F.; Egidi, F.; Goings, J.; Peng, B.; Petrone, A.; Henderson, T.; Ranasinghe, D.; Zakrzewski, V. G.; Gao, J.; Rega, N.; Zheng, G.; Liang, W.; Hada, M.; Ehara, M.; Toyota, K.; Fukuda, R.; Hasegawa, J.; Ishida, M.; Nakajima, T.; Honda, Y.; Kitao, O.; Nakai, H.; Vreven, T.; Throssell, K.; Montgomery, J. A., Jr.; Peralta, J. E.; Ogliaro, F.; Bearpark, M.; Heyd, J. J.; Brothers, E.; Kudin, K. N.; Staroverov, V. N.; Keith, T.; Kobayashi, R.; Normand, J.; Raghavachari, K.; Rendell, A.; Burant, J. C.; Iyengar, S. S.; Tomasi, J.; Cossi, M.; Millam, J. M.; Klene, M.; Adamo, C.; Cammi, R.; Ochterski, J. W.; Martin, R. L.; Morokuma, K.; Farkas, O.; Foresman, J. B.; Fox, D. J.; Gaussian, Inc.: Wallingford, CT, 2016.

(51) Wadt, W. R.; Hay, P. J. Ab Initio Effective Core Potentials for Molecular Calculations. Potentials for Main Group Elements Na to Bi. *J. Chem. Phys.* **1985**, 82, 284–298.

(52) Schlegel, H. B. Optimization of Equilibrium Geometries and Transition Structures. *Adv. Chem. Phys.* **2007**, 67, 249–286.

(53) Smith, P. J.; Tupčiauskas, A. P. Chemical Shifts of ^{119}Sn Nuclei in Organotin Compounds. *Annu. Rep. NMR Spectrosc.* **1978**, 8, 291–370.

(54) Kolb, U.; Draeger, M.; Dargatz, M.; Jurkschat, K. Unusual Hexacoordination in a Triorganotin Fluoride Supported by Intermolecular Hydrogen Bonds. Crystal and Molecular Structures of 1-Aza-5-Stanna-5-Halotricyclo[3.3.3.0^{1,5}]Undecanes $N(CH_2CH_2CH_2)_3SnF \cdot H_2O$ and $N(CH_2CH_2CH_2)_3SnX$ (X = Cl, Br, I). *Organometallics* **1995**, 14, 2827–2834.